Open Journal of Inorganic Chemistry, 2016, 6, 175-182
Published Online July 2016 in SciRes. http://www.scirp.org/journal/ojic
http://dx.doi.org/10.4236/ojic.2016.63013

Scientific Research Publishing

Ellipsometric Study of SiO_x Thin Films by Thermal Evaporation

David Salazar[1], Roberto Soto-Molina[1], Eder German Lizarraga-Medina[1], Marco Antonio Felix[2], Nicola Radnev[2], Heriberto Márquez[1]

[1]Departamento de Óptica, CICESE, Ensenada, México
[2]Instituto de Ingeniería, Universidad Autónoma de Baja California, Mexicali, México
Email: davisa@cicese.mx

Received 20 April 2016; accepted 2 July 2016; published 5 July 2016

Copyright © 2016 by authors and Scientific Research Publishing Inc.
This work is licensed under the Creative Commons Attribution International License (CC BY).
http://creativecommons.org/licenses/by/4.0/

Open Access

Abstract

This paper presents a study of amorphous SiO_x thin films by means of Variable Angle Spectroscopic Ellipsometry (VASE) technique. Tauc Lorentz, Lorentz and Cauchy models have been used to obtain physical thickness and complex refractive index (n and k) from experimental data. In order to obtain a wide range to x stoichiometry values, the films were prepared by vacuum thermal evaporation of SiO on glass substrates, under different and controlled deposition conditions.

Keywords

Ellipsometry, Refraction Index, SiO_x Thin Films

1. Introduction

SiO_x thin films have an important role in new technologies *i.e.* gate dielectric, silicon based light emitters, third generation solar cells, and SOI optical waveguides [1]-[6]. The SiO_x is a material that can be fabricated by different techniques, in particular varying deposition conditions as pressure and evaporation rate when using thermal evaporation, silicon suboxide films with variable stoichiometry (SiO_x, $1 < x < 2$) whose optical properties depend on x value can be obtained [7]-[10]. Structural properties of the silicon oxide films studied by IR absorption and Raman spectra [11] reported that the structure of the films depends significantly on preparation method. Spectroscopic Ellipsometry and Transmission Electron Microscopy were used to obtain the volume fraction, *f*, the pure Si phase in silicon oxide thin films [12]. Variable Angle Spectroscopic Ellipsometry (VASE) is a robust technique based on interaction between film and polarized light, which can be used to determine complex refraction index and thickness of SiO_x films. In order to obtain SiO_x thin film dispersion, it is necessary to consider the film properties (transparency, thickness, rugosity, etc.), and select an appropriate model of dielectric func-

How to cite this paper: Salazar, D., Soto-Molina, R., Lizarraga-Medina, E.G., Felix, M.A., Radnev, N. and Márquez, H. (2016) Ellipsometric Study of SiO_x Thin Films by Thermal Evaporation. *Open Journal of Inorganic Chemistry*, **6**, 175-182.
http://dx.doi.org/10.4236/ojic.2016.63013

tion as Lorentz, Tauc Lorentz and Cauchy models that deserves to be studied; due there are a few works related with SiO_x thin film dispersion curves [13] [14]. In this paper results on dispersion of SiO_x thin films growth with different evaporation rates at different work pressure, obtained by means of VASE technique are presented.

2. Dielectric Function Models

Ellipsometry is an effective method to determine thin film thicknesses and their optical properties. These properties are not directly measured by ellipsometry, but a modeling procedure is needed to extract them from the measured ellipsometric spectra. During the evaluation, the unknown dielectric functions ($\varepsilon = \varepsilon_1 + i\varepsilon_2$) are usually modeled with oscillator function. The oscillator parameters are influenced by the composition and the structure of the material, since these microscopic properties determine the optical, and other physical properties of the film material. This section will explain various dielectric function models including the Lorentz, Cauchy, and Tauc-Lorentz models. Basically, all these models are derived from the Lorentz model [14] [15].

2.1. Lorenz Model

A general and usual approach to fit the dielectric function is to use of Lorentz oscillators, this model assume that the dielectric permittivity can be described by a sum of multiple of resonance Lorentzian functions. This method is often used to have a smooth analytical representation of the dielectric function and is given by,

$$\varepsilon = 1 + \sum_{i=1}^{n} \frac{A_i}{\left(E_{0i}^2 - E^2\right) + i\Gamma_i E} \tag{1}$$

where E denote the photon energy, and E_{0i}^2, A_i, Γ_i are the central photon energy, the amplitude, and the broadening of the ith oscillator, respectively. In Equation (1), the dielectric function is described as the sum of different oscillators [14].

2.2. Cauchy Model

The Sellmeier model originated with the Lorentz model, expressed in terms of wavelengths, and replacing the plasma and resonant frequencies by empirical values. The Sellmeier model corresponds to a region where $\varepsilon_2 \sim 0$ in the Lorentz model and this model can be derived by assuming Γ tends to zero at $\omega \ll \omega_0$, where ω_0 is resonant frequency of the electron. In this condition, if we transform dielectric constant using $\omega/c = 2\pi/\lambda$, we obtain

$$\varepsilon = \varepsilon_1 = 1 + \frac{e^2 N_e}{\varepsilon_0 \left(2\pi c\right)^2 m_e} \frac{\lambda_0^2 \lambda^2}{\lambda^2 - \lambda_0^2} \tag{2}$$

where m_e and e are the mass and charge of the electron, N_e is number of electrons per unit volume, c is speed of light in free space, ε_0 is free space permittivity, ω is angular frequency and λ is wavelength of light.

On the other hand, Cauchy formula is a simplified version of the Sellmeier one, applicable to transparent material or spectral regions far from absorption lines; the Cauchy model is given by

$$n = A + \frac{B}{\lambda^2} + \frac{C}{\lambda^4} + \cdots, \quad k = 0 \tag{3}$$

The above equation can be obtained from the series expansion of Equation (2). Cauchy model is an equation relative to the refractive index n, an approximate function of the Sellmeier model [14].

2.3. Tauc-Lorentz Model

The Tauc-Lorentz oscillator is generally used for amorphous materials, for example for *a-Si* layers. The absorption band in the imaginary part of the dielectric function is defined as:

$$\varepsilon_{2TL}\left(E\right) = \frac{A_{TL} E_{n..TL} B_{TL} \left(E - E_g\right)^2}{E\left(\left(E^2 - E_{n..TL}^2\right)^2 + B_{TL}^2 E^2\right)} \text{ if } E > E_g, \quad \text{and} \quad 0 \text{ if } E \le E_g \tag{4}$$

where A_{TL}, E_{n_TL} and B_{TL}, denotes the amplitude, position, broadening of the TL oscillator, respectively, and E_g is

the band gap. The real part of the dielectric function is calculated using the Kramers-Kronig relation [15].

3. Experimental

The SiO_x thin films were prepared by means of thermal evaporation of silicon monoxide (Balzers SiO 99.5%), on transparent glass substrate, in a BOC Edwards Auto-500 thin film coating system. Spectral transmittance measurements of films were obtained with Stellar Net 2000 spectrophotometer and their ellipsometric characterization (thickness and refraction index measurements) was made by means of a J. A. Woollam M-2000 spectroscopic ellipsometer shown in **Figure 1**, with spectral range from 245 to 1000 nm, at incidence angles of 55˚, 65˚ and 75˚. It is known that SiO_x films growth by thermal evaporation have an amorphous random network of tetrahedral coordinated silicon and oxygen and its stoichiometry is a function of the oxygen partial pressure and evaporation rate [10].

In this work, SiO_x thin films were deposited in a room temperature substrate (~30˚C), varying the evaporation rate and vacuum pressure of the chamber. A main goal is to modify films stoichiometry by different deposition rates, at two vacuum pressures: low vacuum ~10^{-4} Torr and high vacuum ~10^{-6} Torr. **Table 1** shows evaporation parameters of the thin films, included thickness values obtained from quartz microbalance SQM Infinicom thin film deposition monitor. The source material SiO was evaporated from Tantalum boat using at a controlled deposition rate.

4. Results and Discussion

The fabrication conditions are expected to influence the optical properties of SiO_x films, this section presents results of dispersion and transmission of SiO_x thin films.

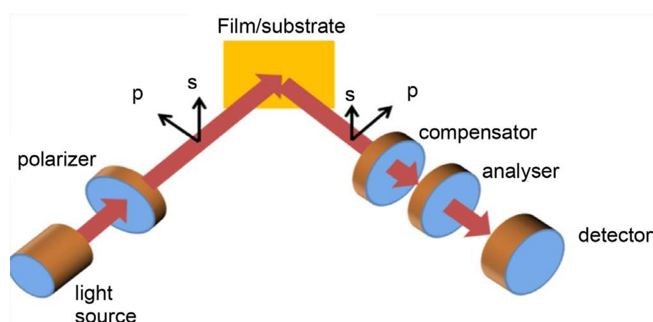

Figure 1. Main components of a variable angle spectroscopic ellipsometer (VASE).

Table 1. Evaporation parameters of SiO_x films.

No.	Evaporation Rate (nm/s)	Initial Vacuum (Torr)	Final Vacuum (Torr)	Thickness (nm)
1	0.3	~10^{-4}	~10^{-4} - ~10^{-4}	304
2	0.6	~10^{-4}	~10^{-4} - ~10^{-4}	233
3	0.9	~10^{-4}	~10^{-4} - ~10^{-4}	306
4	1.2	~10^{-4}	~10^{-4} - ~10^{-4}	220
5	1.5	~10^{-4}	~10^{-4} - ~10^{-4}	306
6	0.35	~10^{-6}	~10^{-6} - ~10^{-5}	493
7	0.65	~10^{-6}	~10^{-6} - ~10^{-5}	556
8	0.65	~10^{-6}	~10^{-6} - ~10^{-5}	556
9	0.95	~10^{-6}	~10^{-6} - ~10^{-5}	405
10	1.5	~10^{-6}	~10^{-6} - ~10^{-6}	264
11	2.0	~10^{-6}	~10^{-6} - ~10^{-7}	524

4.1. Transmission of SiO_x Thin Films

Figure 2 shows spectral transmittance of SiO_x thin films fabricated a different evaporation rate, from 300 *nm* to 1100 nm range. Films obtained at low vacuum pressure have similar spectrums with a slightly decrease in transmission for higher evaporation rates, see **Figure 2(a)**. On the other hand, spectral transmittance shown in **Figure 2(b)**, obtained at high vacuum pressure, have the typical interference oscillations related to thin film thickness; from which more oscillations appears when increase film thickness [16]. Spectral transmission curves of SiO_x films, presented in **Figure 2**, exhibit a transmission shift towards longer wavelengths; this shift can be associated to the amount of silicon (Si) in the film [8]. The spectral transmission of SiO_x films, that had values of x close to 2, approaches to SiO_2 spectrum, as expected. Otherwise when stoichiometry value of SiO_x films is x close to 1, spectrum approaches to the SiO. Clearly, we can observe that when evaporation rate increase, transmittance curve have a shift towards higher wavelengths as consequence of more *Si* presence in SiO_x films.

4.2. Ellipsometry of SiO_x Thin Films

Here is considered that SiO_x stoichiometry ($1 < x < 2$) can be tuned by means of evaporation rate of the film during the deposition process. The ellipsometry provides information of the refractive index dispersion curves and the physical thickness by means of polarization state changes described as the ratio (Ψ) between the amplitude reflection coefficients r_p and r_s and the difference between their phases (Δ). There are several models that use dispersion relations to obtain the thickness and the refractive index (real part n and imaginary part k). Normally, experimental data of Ψ and Δ in spectral range are compared and adjusted with values of a particular model. Model parameters are adjusted to fit closely experimental and theoretical data. The fitting process includes a choice of initial values for the unknown parameters and the minimization of the function *MSE* (*MSE* mean squared error) by subsequent iterations [17].

MSE function, which is essentially the sum of the squares of the differences between the measured and calculated data for each (Δ, Ψ) pair, is given by

$$MSE = \sqrt{\frac{1}{2N-M}\left[\left[\sum_{i=1}^{N}\frac{\psi_i^{Theo}-\psi_i^{Exp}}{\sigma_{\psi,i}^{Exp}}\right]^2+\left[\sum_{i=1}^{N}\frac{\Delta_i^{Theo}-\Delta_i^{Exp}}{\sigma_{\Delta,i}^{Exp}}\right]^2\right]} \quad (5)$$

where N is the number of measured Ψ and Δ pairs, M is the total number of variable parameters and σ is the standard deviations. The superscript *Theo* means theoretical model and the *Exp* means the experimental data. Nevertheless, obtaining a low *MSE* does not guarantee accurate thicknesses and optical constants.

Films that have a refractive index that varies with depth can be approximated as a set of layers, each one with an individual refraction index value. Furthermore, surface roughness can be taken account using the Bruggeman effective medium approximation (*EMA*) [18]. Physical interpretation of *EMA* theory involves small particles of one material suspended within a host material. Under this approximation, the optical constants can be mixed to satisfy

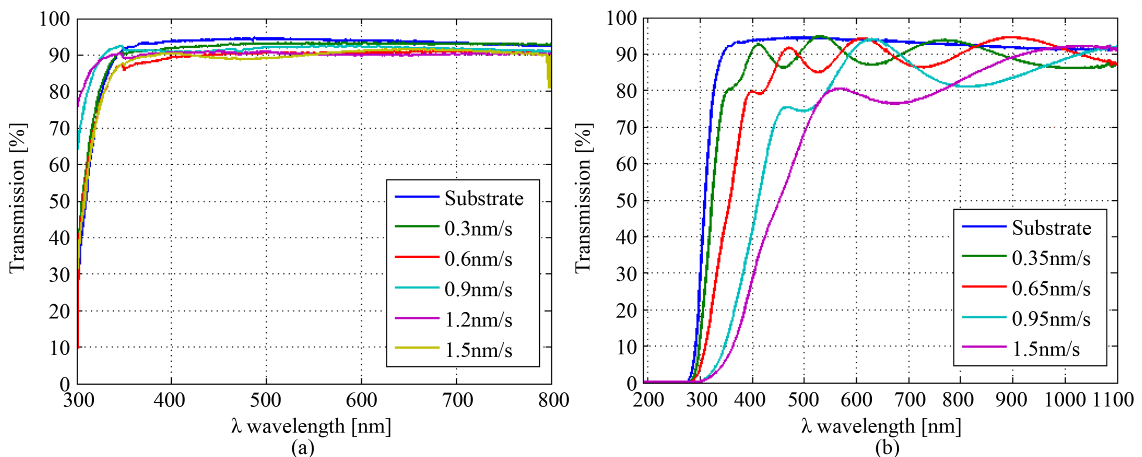

Figure 2. Spectral transmittance of SiO_x film evaporated under: (a) low vacuum and (b) high vacuum.

electromagnetic equations: the Lorentz Lorenz equation for a mixture of material whose complex dielectric constants and volume fractions are ε_i and f_i, and the Bruggeman formula for computing ε in terms of ε_i and f_i is,

$$0 = \sum_i f_i \frac{\varepsilon_i - \varepsilon}{\varepsilon_i + 2\varepsilon} \tag{6}$$

In this model, a single, planar layer, with thickness varying to provide the best approximation of the surface properties, can represent roughness.

The ellipsometry software Complete EASE (J. A. Woollam Co., Inc.) was used to fit experimental and theoretical spectroscopy ellipsometry curves. With this software it is possible to select a physical model and fit with data acquired by means spectroscopic ellipsometry. A diffuse tape was used on substrate backside to eliminate or reduce secondary reflection, which can be a noise signal during measurements. **Figure 3** shows dispersion curves obtained for substrate from 250 to 1000 nm with mean square error *MSE* of 1.88 and surface roughness of 2.7 nm.

During the fitting process, first SiO_x samples were characterized by B-spline or Cauchy model, and with these initial values a second fitness process is realized using other models that have physical significance. In our work, Cauchy, Lorentz, and Tauc-Lorentz models were used due that are more appropriate to amorphous materials. Here, to obtain a better fit, a graded layer, with ten slices, was considered. Typical spectroscopic ellipsometry data for a SiO_x film are shown in **Figure 4**. In this case, SiO_x film was deposited at 0.35 nm/s and **Figure 4(a)** shows a fit with Cauchy model with values of *MSE* = 22.78, thickness 456.20 ± 0.48 nm and rugosity of 2.65 ± 0.13 nm and **Figure 4(b)** includes a gradient structure of the film with values *MSE* = 19.60, thickness 453.19 ± 0.43 nm and rugosity of 1.96 ± 0.12 nm. **Figure 4(c)** shows a fit for a SiO_x film deposited at 0.35 *nm/s* using Lorentz model with *MSE* = 9.41, thickness 461 ± 0.23 *nm* and rugosity of 1.49 ± 0.06 nm and **Figure 4(d)** include a gradient structure of the film with *MSE* = 7.44, thickness 450.19 ± 0.54 nm and rugosity of 0.43 ± 0.07 nm.

Table 2 show results of calculated refractive indices for SiO_x films using different models. Cauchy and Lorentz models were used to fit SiO_x films obtained with low vacuum evaporation process, and Lorentz and Tauc-Lorentz models were used to fit SiO_x films obtained with high vacuum evaporation process.

Figure 5 shows dispersion curves for SiO_x films evaporated with different deposition conditions, presented in **Table 1**. From the last results, it is possible to note the influence of evaporation parameters on dispersion curves. In particular, SiO_x films obtained at low vacuum condition have refractive index in the range of n ~ 1.4 - 1.53, and films obtained at high vacuum condition have higher values of refractive index *i.e.* n ~ 2.0. The evaporation rate has a notable influence on dispersion curves, and their contribution is described below. In general, we can observe little discrepancies on dispersion curves obtained from the different used models. B-spline model do not have a physical meaning and Cauchy Model is used on transparent films modeling. In order to obtain a best description of dispersion curves, a Lorentz model (oscillators) and Tauc-Lorentz (considering oscillators and density of states) models were used, including a refraction index gradient supposition.

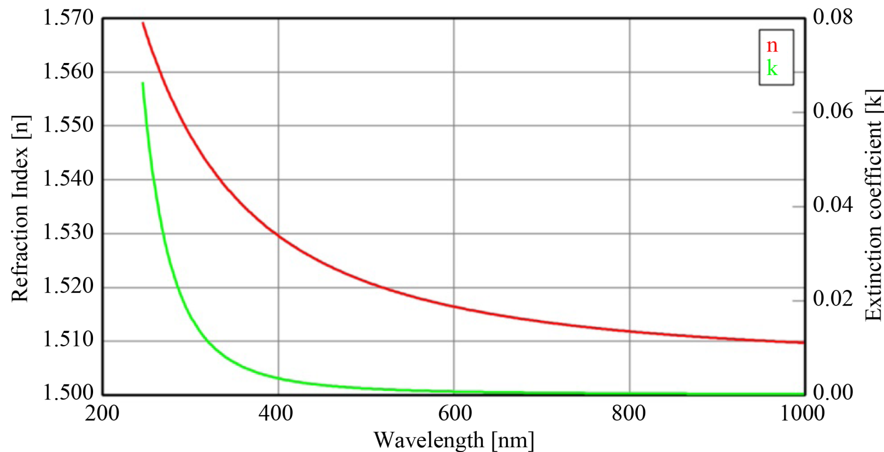

Figure 3. Dispersion curves of glass substrate.

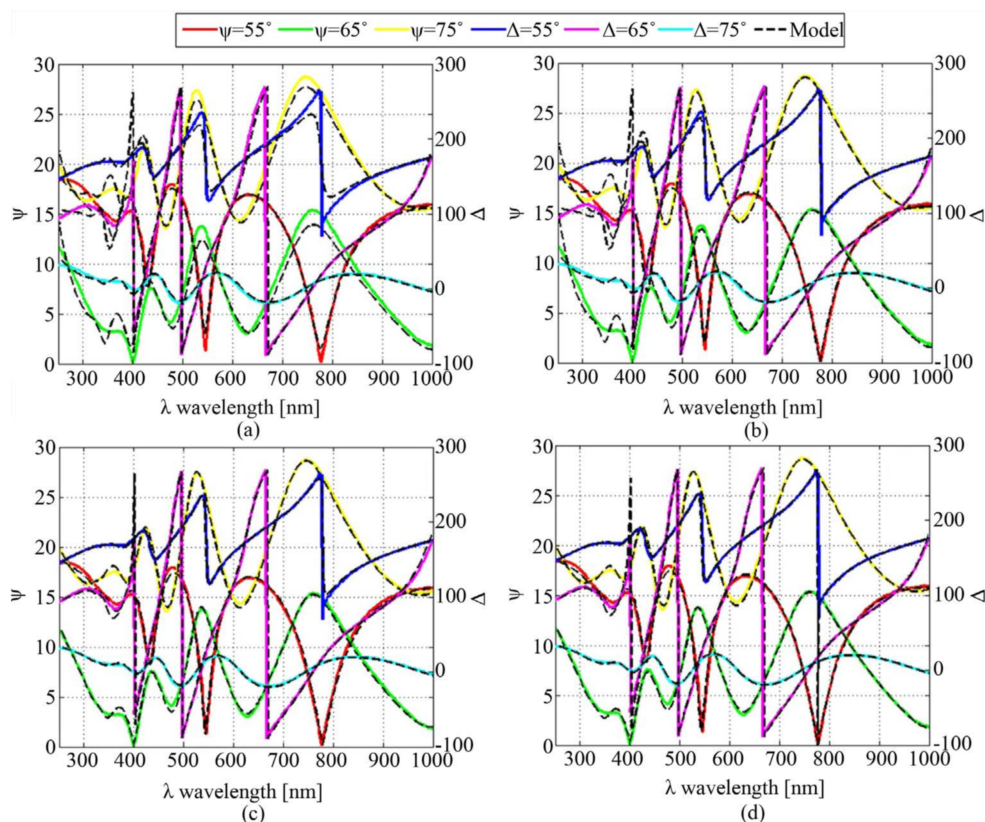

Figure 4. Fitted ellipsometric parameters Ψ and Δ of No. 6 sample using the Cauchy: (a) no gradient included, (b) gradient included; and Lorentz model: (c) no gradient included, (d) gradient included.

Table 2. Calculated refraction index for SiO_x films obtained with different models at $\lambda = 633$ nm.

No.	Rate (nm/s)*	Refraction Index*	Refraction Index*	Extinction Coefficient*
1	0.3^{Lv}	1.4191^{C}	1.4191^{L}	0.0^{C}
4	1.2^{Lv}	1.4633^{C}	1.4433^{L}	0.0^{C}
5	1.5^{Lv}	1.4720^{C}	1.4552^{L}	0.0^{C}
6	0.35^{Hv}	1.6427^{T-L}	1.6243^{L}	0.23×10^{-3C}
7	0.65^{Hv}	1.6780^{T-L}	1.6758^{L}	0.57×10^{-3C}
9	0.95^{Hv}	1.8117^{T-L}	1.7975^{L}	0.91×10^{-2C}
10	1.5^{Hv}	1.9873^{T-L}	1.9441^{L}	0.52×10^{-1C}
11	2^{Hv}	1.9474^{T-L}	1.9474^{L}	0.11×10^{-1C}

Note*: Lv is Low vacuum, Hv is high vacuum, C is Cauchy model, L is Lorentz model, and T-L is Tauc-Lorentz model.

From dispersion curves shown in **Figure 5** for SiO_x films, it is possible to see a relationship between refractive index of the films and their evaporation rates; refraction index increase as evaporation rate increase**.** Previous works on the synthesis of SiO_x films, have shown a direct relation between the stoichiometry x and the refractive index of the films [7]-[10].

Figure 6 shows the refraction index of SiO_x films at 633 *nm* as a function of evaporation rate, when deposited with high vacuum process of about ~10^{-6} Torr. Refractive index values of SiO_x films have values in a range from 1.6 - 1.95; higher *n* values were obtained at higher evaporation rate, as is expected. At higher evaporation rates, the oxidation in the films is avoided and therefore approach to the stoichiometry and refractive index of

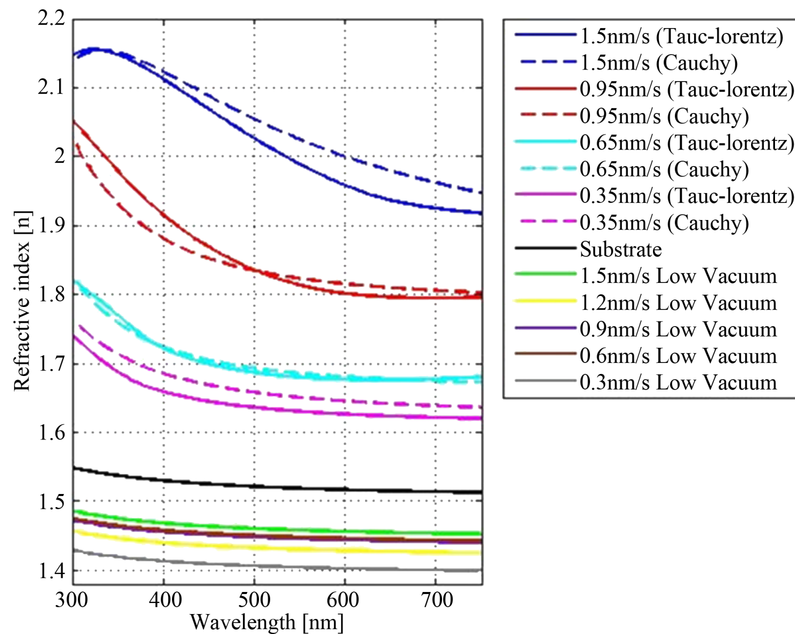

Figure 5. Dispersion curves obtained with VASE to films prepared by different deposition rate.

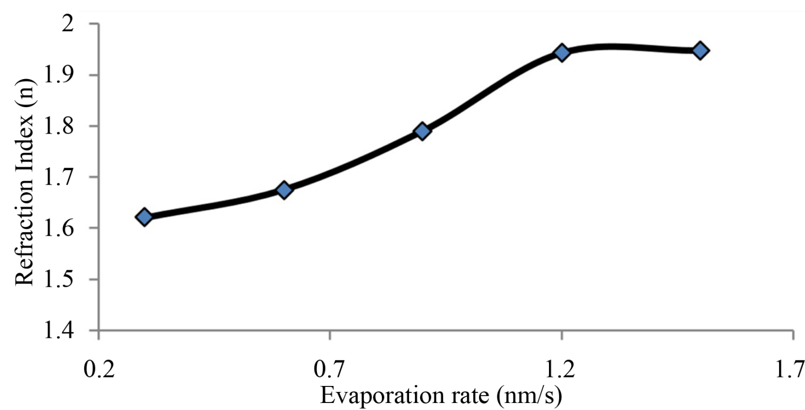

Figure 6. Refraction index (*n*) in function of evaporation rate at 10^{-6} Torr and λ = 632.8 nm.

SiO films with x = 1. However, refractive index of SiO_x films evaporated with low vacuum process of about ~10^{-4} Torr has lower values of *n* ~ 1.45 which is close to a SiO_2 stoichiometry with x = 2. When the vacuum in the chamber is low, the film tends to oxide even for high evaporation rates. Furthermore, it can be appreciated that for higher evaporation rates (*i.e.* 1.5 nm/s) a higher refractive index is obtained, even at this vacuum. From the results presented it is possible to foresee the potential of modulation of refractive index of SiO_x films as function of evaporation rate and vacuum pressure for application in integrated optical devices.

5. Conclusion

SiO_x thin films have been obtained by thermal evaporation of SiO under low vacuum (~10^{-4} Torr) and high vacuum (~10^{-6} Torr) with different rates of evaporation from 0.35 to 2 nm/sec. Spectroscopic ellipsometry analysis of thin films was done by fitting experimental data of Ψ and Δ pairs with Lorentz, Tauc Lorentz and Cauchy models, showing little discrepancies and good agreement on dispersion curves obtained from the different used models. Dispersion curves of SiO_x thin films indicate that it is possible to modulate refractive index of SiO_x in a range of 1.42 to 1.95 at 633 nm as function of evaporation rate and vacuum pressure.

Acknowledgements

The authors would like to thank J. L. Angel-Valenzuela and J. Davalos for their technical support. R. Soto would like thanks to scholarship Grant CONACYT No. 369368.

References

[1] Yao, J., Lin, J., Dai, Y., Ruan, G., Yan, Z., Li, L., Zhong, L., Natelson, D. and Tour, J.M. (2012) Highly Transparent Nonvolatile Resistive Memory Devices from Silicon Oxide and Graphene. *Nature Communications*, **3**, Article ID: 1101. http://dx.doi.org/10.1038/ncomms2110

[2] Wang, G., Raji, A.R., Lee, J.H. and Tour, J.M. (2014) Conducting-Interlayer SiO_x Memory Devices on Rigid and Flexible Substrates. *ACS Nano*, **8**, 1410-1418. http://dx.doi.org/10.1021/nn4052327

[3] Kakiuchi, H., Ohmi, H., Yamada, T., Tamaki, S., Sakaguchi, T., Lin, W.C. and Yasutake, K. (2015) Characterization of Si and SiOx Films Deposited in Very High-Frequency Excited Atmospheric-Pressure Plasma and Their Application to Bottom-Gate Thin Film Transistors. *Physica Status Solidia*, **212**, 1571-1577. http://dx.doi.org/10.1002/pssa.201532328

[4] Mazzarella, L., Kirner, S., Gabriel, O., Korte, L., Stannowski, B., Rech, B. and Schlatmann R. (2015) Nanocrystalline Silicon Oxide Emitters for Silicon Hetero Junction Solar Cells. *Energy Procedia*, **77**, 304-310. http://dx.doi.org/10.1016/j.egypro.2015.07.043

[5] Littlejohns, C.G., Nedeljkovic, M., Mallinson, C.F., Watts, J.F., Mashanovich, G.Z., Graham T. Reed, G.T. and Gardes, F.Y. (2015) Next Generation Device Grade Silicon-Germanium on Insulator. *Scientific Reports*, **5**, Article ID: 8288. http://dx.doi.org/10.1038/srep08288

[6] Subbaraman, H., Xu, X., Hosseini, A., Zhang, X., Zhang, Y., Kwong, D., Ray, T. and Chen, R.T. (2015) Recent Advances in Silicon-Based Passive and Active Optical Interconnects. *Optics Express*, **23**, 2487-2511. http://dx.doi.org/10.1364/OE.23.002487

[7] Pivot, J. (1982) Mechanical Properties of SiOx Thin Films. *Thin Solid Films*, **89**, 175-190. http://dx.doi.org/10.1016/0040-6090(82)90446-1

[8] Shabalov, A.L. and Feldman, M.S. (1983) Optical and Dielectric Properties of Thin SiOx Films of Variable Composition. *Thin Solid Films*, **110**, 215-224. http://dx.doi.org/10.1016/0040-6090(83)90239-0

[9] Zuther, G., Hübner, K. and Rogmann, E. (1979) Dispersion of the Refractive Index and Chemical Composition of SiOx Films. *Thin Solid Films*, **61**, 391-395. http://dx.doi.org/10.1016/0040-6090(79)90485-1

[10] Tomozeiu, N. (2011) Silicon Oxide (SiO_x, $0 < x < 2$): A Challenging Material for Optoelectronics. In: Predeep, P., Ed., *Optoelectronics—Materials and Techniques*, InTech, 56-98.

[11] Nikitin, T. and Khriachtchev, L. (2015) Optical and Structural Properties of Si Nanocrystals in SiO_2 Films. *Nanomaterials*, **5**, 614-655. http://dx.doi.org/10.3390/nano5020614

[12] Mateos, D., Curiel, M.A., Nedev, N., Nesheva, D., Machorro, R., Manolov, E., Abundiz, N., Arias, A., Contreras, O., Valdez, B., Raymond, O. and Siqueiros, J.M. (2013) TEM and Spectroscopic Ellipsometry Studies of Multilayer Gate Dielectrics Containing Crystalline and Amorphous Si Nanoclusters. *Physica E*, **51**, 111-114. http://dx.doi.org/10.1016/j.physe.2012.11.015

[13] Tauc, J. (1969) Optical Properties and Electronic Structure of Amorphous Semiconductors. In: Nudelmre, S. and Mitra S.S., Eds., *Optical Properties of Solids*, Springer, New York, 123-136. http://dx.doi.org/10.1007/978-1-4757-1123-3_5

[14] Fujiwara, H. (2008) Spectroscopic Ellipsometry: Principles and Applications. Wiley, England.

[15] Budai, J., Hanyecz, I., Szilágyi, E. and Tóth, Z. (2011) Ellipsometric Study of Si_xC Films: Analysis of Tauc-Lorentz and Gaussian Oscillator Models. *Thin Solid Films*, 2985-2988. http://dx.doi.org/10.1016/j.tsf.2010.12.073

[16] Macleod, H.A. (2001) Thin-Film Optical Filters. CRC Press, London. http://dx.doi.org/10.1201/9781420033236

[17] Woollam, J.A., Snyder, P.G. and Rost, M.C. (1988) Variable Angle Spectroscopic Ellipsometry: A Non-Destructive Characterization Technique for Ultrathin and Multilayer Materials. *Thin Solid Films*, **166**, 317-323. http://dx.doi.org/10.1016/0040-6090(88)90393-8

[18] Bosch, S., Ferré-Borrull, J., Leinfellner, N. and Canillas A. (2000) Effective Dielectric Function of Mixtures of Three or More Materials: A Numerical Procedure for Computations. *Surface Science*, **453**, 9-17. http://dx.doi.org/10.1016/S0039-6028(00)00354-X

Submit or recommend next manuscript to SCIRP and we will provide best service for you:

Accepting pre-submission inquiries through Email, Facebook, Linkedin, Twitter, etc
A wide selection of journals (inclusive of 9 subjects, more than 200 journals)
Providing a 24-hour high-quality service
User-friendly online submission system
Fair and swift peer-review system
Efficient typesetting and proofreading procedure
Display of the result of downloads and visits, as well as the number of cited articles
Maximum dissemination of your research work

Submit your manuscript at: http://papersubmission.scirp.org/